The quorum-sensing lexicon of *Salmonella* ameliorates acid stress in the host by a non-canonical mechanism

Anmol Singh[a], Abhilash Vijay Nair[a,e,#], Shashanka Aroli[a#], Suman Das[b], Subhrajit Karmakar[b], R. S. Rajmani[c], Santanu Mukherjee[b], Umesh Varshney[a], Dipshikha Chakravortty[a,d]*

[a]Department of Microbiology and Cell Biology, Division of Biological Sciences, Indian Institute of Science, Bengaluru, India

[b]Department of Organic Chemistry, Indian Institute of Science, Bengaluru, India

[c]Molecular Biophysics Unit, Indian Institute of Science, Bengaluru, India

[d]Adjunct Faculty, School of Biology, Indian Institute of Science Education and Research, Thiruvananthapuram, India

[e]Present address: Department of Microbiology and Immunology, Vagelos College of Physicians and Surgeons, Columbia University, New York, NY 10032, USA

*Corresponding author: dipa@iisc.ac.in,

[#]These authors contributed equally.

Tel: +91 80 2293 2842,

Fax: +91 80 2360 2697

Abstract

The intestinal milieu is largely characterized by the complex array of chemical compounds produced through the metabolic activity of resident microbiota. Enteric pathogens like *Salmonella*, which have evolved refined mechanisms to persist within this environment, utilize these microbial metabolites and self-produce quorum molecules as molecular cues to identify ecological niches and modulate their survival and virulence strategies. *Salmonella* quorum sensing involves producing and detecting Autoinducer-2 (AI-2) signaling molecules. Our research reveals that *Salmonella* Typhimurium enhances AI-2 biosynthesis and transport under acidic conditions, aiding environmental adaptation and facilitating pathogenesis in macrophages. AI-2 signaling regulates the pH-sensing two-component system genes, *phoP/phoQ*, ensuring cytosolic pH homeostasis, survival, and acid tolerance. It also involves regulating the lysine/cadaverine-mediated acid tolerance response and maintaining bacterial cytosolic pH. Furthermore, we show that the repressor LsrR protein, apart from the *lsr* promoter, binds to only one strand of the *phoP* promoter via its Y25 and R43 amino acids to negatively modulate *phoP* expression. Additionally this signaling ameliorates the intracellular survival by modulating *Salmonella* Pathogenicity Island-2 (SPI-2) regulators (*ssrA/ssrB*) and SPI-2 effector expression via PhoP. Mouse models demonstrate that AI-2 signaling is essential for colonizing the primary and secondary infection sites, showcasing its critical role in pathogenesis and low pH survival mechanisms in *Salmonella*.

Keywords: Autoinducer-2, acidic pH, macrophage, PhoP/PhoQ, *Salmonella* pathogenicity island-2

Introduction

Salmonella is considered a major foodborne enteric pathogen worldwide (1), and it gains access to the host through contaminated food and water. The bacteria stealthily survive the acidic pH of the stomach and the hostile environment of the host macrophages. Within the host cells, *Salmonella* resides in the *Salmonella*-containing vacuole (SCV), a membrane-bound compartment that provides with an acidic niche facilitating utilization of the SPI-2 encoded genes for the intracellular proliferation of the bacterium (2-4). *Salmonella enterica* serovars infection in humans can elicit a wide range of clinical outcomes, spanning asymptomatic carriage, acute self-limiting gastroenteritis, invasive systemic disease with associated bacteremia, and enteric (typhoid) fever(5).

The community behaviour of bacteria, known as quorum sensing, protects them from various stress factors such as exposure to ultraviolet light, acids, detergents, or antimicrobial agents (6, 7). Also, AI-2 signaling is linked to bacterial survival and pathogenesis, for example, in *Lactobacillus sp.,* AI-2 helps in survival under acidic conditions (8, 9). *Salmonella* recognizes a chemically distinct quorum sensing signal called autoinducer 2 (AI-2), synthesized by the enzyme LuxS (10), which is maximally produced during its exponential growth phase (11). As bacterial quorum increases, extracellular AI-2 accumulates and, upon reaching a threshold, it is sensed by LsrB protein in *Salmonella*. AI-2 is then transported into the cytosol by an ABC transporter (LsrA, LsrB, LsrC, and LsrD) encoded by the *lsr* operon and phosphorylated by the LsrK kinase. The phosphorylated AI-2 binds LsrR repressor protein, and relieves the LsrR mediated repression of the *lsr* operon to enable further import of AI-2 (12, 13).

The LuxS/AI-2 signaling regulates the expression of oxidative stress response related genes such as *sodA*, *sodCI*, and *sodCII* , which play an essential role in survival of *Salmonella* within macrophages (14). Further, the release of LsrR from DNA by AI-2 is essential for SPI-1 transcription and flagella expression in *Salmonella* (15, 16). However, the molecular basis of this remains unclear, not only because of the diverse and distinct survival strategies of *Salmonella* but also due to the limited understanding of the AI-2 regulatory mechanism and its role in enhancing pathogenesis beyond the *lsr* operon.

As an enteric pathogen, *Salmonella* has to thrive in diverse and competitive environments in the gastrointestinal tract. It needs to sense and adapt to a variety of environmental barriers such as host physiology, nutrient availability, osmotic stress, and competition with other gut bacteria(17). Counteracting and conquering the acidic pH of the stomach and acidic intravacuolar environment is an indispensable survival strategy for *Salmonella*. We contemplated that the interbacterial communication and signaling systems might control the pH sensing and tolerance responses. Here, we show that LuxS/AI-2 signaling regulates a two-component system *phoP*/*phoQ* to activate the acid tolerance system in *Salmonella* and tune the SPI-2 encoded genes, enhancing its survival in *in vitro* and *in vivo* models. We found that LsrR, the regulator of LuxS/AI-2 signaling, binds to the *phoP/phoQ* promoter via its Y25 and R43 amino acid residues, apart from its known regulation of the *lsr* operon. This way, LuxS/AI-2 coordination facilitates dynamic changes of the *Salmonella* transcriptome according to the surrounding environment and promotes rapid adaptation to different environmental niches to increase population fitness.

Materials and Methods

Bacterial strains and Growth conditions-

The wild-type *Salmonella enterica* serovar Typhimurium strain 14028S (STM WT) used in all experiments in this study was a kind gift from Professor Michael Hensel of the Max Von Pettenkofer-Institute for Hygiene und Medizinische Mikrobiologie in Germany. The bacterial strains were revived on LB agar with or without antibiotics. The LB broth culture of wild-type, knockout, and complemented strains was cultured at 37˚C (170 rpm) in an orbital shaker incubator. Antibiotics Kanamycin (50µg/ml), Chloramphenicol (25µg/ml), and Ampicillin (50µg/ml) were used wherever required. *Vibrio campbellii* ATTC BAA-1117 strain was used for autoinducer (AI-2) bioassay. This strain was grown in ATCC Medium: 2746 Autoinducer Bioassay (AB) Medium.

A growth kinetics study was conducted in LB and M9 minimal media (47) (48) (**Table S2**). Briefly, STM WT and mutants were inoculated in fresh LB broth (1:100 ratio from overnight primary culture). The cultures were incubated at 37˚C (170 rpm) in an orbital shaker incubator. The OD at 600nm was measured at regular intervals until 24 hours post-inoculation.

Bacterial gene knockout and strain generation

Salmonella enterica serovar Typhimurium strain 14028S and isogenic mutants were used for all assays. *luxS*, *lsrB*, *lsrK,* and *lsrR* gene knockout strains were made by λ-Red recombination system as described previously in one gene step chromosomal gene inactivation method demonstrated by Datsenko and Wanner (49). Briefly, STM WT strains were transformed with pKD46 plasmid expressing λ-red recombinase system under Arabinose inducible plasmid. The pKD3 and pKD4 plasmid were used as the template

127 to amplify the chloramphenicol and kanamycin resistance cassette with
128 knockout primers **(Table S3).** The amplified reaction products were purified
129 using chloroform isopropanol precipitation. The purified PCR product was
130 transformed into pKD46- containing STM WT expressing λ-Red recombinase
131 system. The transformed cells were plated on LB agar with chloramphenicol
132 and kanamycin accordingly. The knockout strains were confirmed by PCR
133 using primers **(Table S3)** corresponding to the regions ~100bp upstream and
134 downstream of the relevant genes.

135 For complement strain, colony PCR amplified the *luxS* gene with gene-
136 specific primers (containing BamH1 and HindIII restriction site sequence)
137 (Table S3). The amplified PCR product was purified by chloroform
138 isopropanol precipitation and cloned into the empty pQE60 vector using
139 BamH1 and HindIII sites. The double-digested insert and vector were
140 subjected to ligation by T4DNA ligase in ligation buffer (NEB) overnight at
141 16°C. The respective ligated vector was transformed into the STM Δ*luxS*
142 strains to generate the complemented strain. Complement strain was
143 initially confirmed by colony PCR with cloning primers and internal primers
144 of the genes, and finally by restriction digestion of recombinant plasmid
145 isolated from complement strains to study insert release.

146 **Cell culture and maintenance**

147 Murine macrophage cell line RAW 264.7 was maintained in Dulbecco's
148 Modified Eagle Medium (DMEM, Lonza), supplemented with 10% FBS
149 (Gibco) and 1% penicillin-streptomycin (Sigma-Aldrich) in a humidified
150 incubator with 5% CO_2 at 37 °C. The cells were seeded into the respective
151 cell culture plate for each experiment to conduct intracellular survival
152 assays and intracellular gene expression experiments.

Peritoneal macrophage isolation

The primary macrophage isolation was performed as previously described (50). Briefly, C57BL/6J mice (5-6 weeks old) were injected with Brewer's thio-glycolate medium (8% w/v, HIMEDIA). At four days of treatment, 5 ml of cold PBS was injected into the peritoneal cavity, followed by aspiration of the fluid from the cavity and dispensed into a 15 ml centrifuge tube. The centrifugation was done at 300g for 10 min, and the resuspended cell pellet [in Roswell Park Memorial Institute 1640 (RPMI 1640)] was supplemented with 10% FBS and an antibiotic cocktail (penicillin-streptomycin). Cells were counted by hemocytometer and seeded onto 24 well cell culture plates.

Chemical synthesis of acetonide-protected (*S*)-4,5-dihydroxy-2,3-petanedione (DPD)

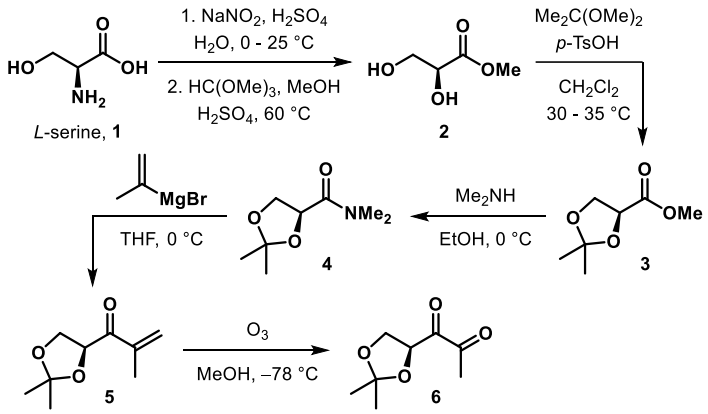

Acetonide-protected DPD **6** was synthesized from commercially available *L*-serine **1** in five steps (for details, see the supplemetary Information). These steps include stereoretentive displacement of the amino group of *L*-serine through diazotisation and esterification to form methyl (*S*)-2,3-dihydroxypropanoate **2** (51) followed by protection of 1,2-diol as acetonide (**3**(52). Transformation of methyl ester of **3** to *N*,*N*-dimethyl amide **4** (53) paved the way for its conversion to isopropenyl ketone **5** by reacting with

174 isopropenyl Grignard reagent. Ozonolytic cleavage of the alkene in **5**
175 resulted in acetonide-protected (*S*)-DPD **6**(54).

176 **AI-2 bioassay**

177 The culture of *Salmonella* Typhimurium WT and mutants was obtained at 0h,
178 1h, 3h, 6h, 9h, and 12h, and centrifuged at 6000rpm for 10 min. After
179 filtration using a 0.22 µm filter, the supernatant was stored at -20 °C until
180 required. The AI-2 was quantified using the sensor strain *Vibrio campbellii*
181 ATTC BAA-1117 (strain designation *V. harveyi* BB-170, which only responds
182 to AI-2). The AI-2 bioassay was performed as previously described (55) (6)
183 with minor modifications. A single colony of *V. harveyi* BB-170 was
184 incubated in 5 ml of Autoinducer Bioassay medium (ATCC Medium: 2746 AB
185 Medium) at 30°C and 200 rpm. A 1:1000 dilution was obtained by
186 transferring a 10 µl sensor strain culture to 10 mL of fresh AB media.
187 *Salmonella* cell-free culture supernatant (20 µl) was incubated with a 180
188 ml diluted sensor strain. The mixture was added to a white, flat-bottomed
189 96-well microtiter plate (Corning, USA), followed by shaking in a rotary
190 shaker at 200 rpm, at 30°C. Luminescence was measured at 3 h in a
191 fluorescent microtiter plate reader. Autoinducer signal calculated as –
192 (luminescence produced by *Vibrio* in the presence of *Salmonella*
193 Typhimurium free supernatant - luminescence in media control)/
194 luminescence produced by *Vibrio* with sterile media. To validate the activity
195 of exogenous DPD molecule and BF-8 inhibitor, an autoinducer bioassay
196 was performed in the presence of DPD and BF-8 inhibitors (Cat# 53796,
197 purchased from Sigma).

198 **Gentamicin protection assay**

199 RAW 264.7 macrophages and peritoneal macrophages isolated from
200 C57BL/6J mice were seeded in tissue culture plates for infection. Cells were
201 infected with STM WT, STM Δ*luxS,* STM Δ*lsrB,* STM Δ*lsrK,* STM Δ*lsrR,* and
202 *STMΔluxS:luxS* (stationary phase culture growing overnight in LB broth). The
203 Multiplicity of Infection (MOI) of 10 was used for the intracellular survival
204 assay. MOI of 20 was used for the *Salmonella* Typhimurium gene expression
205 study (qRT-PCR). Following the infection of STM strains into the cell line, the
206 plate was spun for 5 min at 600 rpm using a Rota-Superspin R–NV swing
207 bucket centrifuge. The plate was then incubated for 25 min at 37 °C with 5%
208 CO_2 in a humidified incubator. The infected cells were washed twice with 1X
209 PBS and treated with a 100 µg/ mL concentration of gentamycin. After 1 h,
210 the media were changed with a reduced concentration of gentamycin (25 µg/
211 mL) and incubated until the desired time point. The time points of 2h, 6h,
212 and 16h were taken for the qRT-PCR samples and 2h and 16h for the
213 intracellular survival assay.

214 Also, for studying the effect of exogenous DPD in the recovery of the
215 phenotype of mutant *luxS,* were grown *in vitro* with supplementation of 25
216 µM, 50 µM,100 µM, and 200 µM DPD molecule and 10%, 20%, 30%, and 50%
217 spent media of STM WT collected at 3h in LB growing. For inhibition, the
218 inhibitor (Z)-4- bromo-5-(bromomethyllene)-3-methylfran-2(5H) known as
219 BF-8 treatment, was added to STM WT in LB media. DPD or spent media
220 supplemented and BF-8 treated culture was used for gentamycin protection
221 assay.

222 **Intracellular survival assay and phagocytosis assay**

223 The cells were lysed with 0.1% triton-X 100 in PBS at specific time points
224 post-infection. For the intracellular survival assay, 2h and 16h post-infection

225 samples were collected and plated, and the corresponding CFU at 2h and
226 16h was determined. Fold proliferation was determined using the formula [
227 CFU at 16 h]/ [CFU at 2 h]. For phagocytosis, the bacterial number was
228 determined in the inoculum and 2h time point post-infection. Percent
229 phagocytosis was by using the formula- (CFU at 2 h)/ (CFU of pre-
230 inoculum)]×100**.**

231 **Confocal microscopy**

232 To study the *Salmonella* proliferation and their intracellular vacuolar status,
233 all STM strains (STM WT, STM Δ*luxS,* STM Δ*lsrB,* STM Δ*lsrK,* and STM Δ*lsrR*)
234 were transformed with pFPV 25.1-mCherry-Amp^R plasmid, and used to
235 infect RAW264.7 cells. Briefly, 1×10^5 RAW264.7 cells were seeded on the
236 coverslip and infected with different strains of bacteria at MOI 25. After
237 appropriate post-infection durations, cells were washed twice with PBS and
238 fixed with 3.5% paraformaldehyde (PFA), and incubated with a specific
239 antibody (anti-mouse LAMP-1) in a blocking buffer containing 2% BSA and
240 0.01% saponin for 2 hours at RT or overnight at 4℃. The cells were washed
241 twice with PBS and incubated with appropriate secondary antibody tagged
242 with fluorochrome for 1 hour at RT. The coverslips were then mounted onto
243 a clean glass slide and imaged under a confocal microscope (Zeiss LSM-
244 710) using a 63X objective.

245 ***In vitro* Cell culture competition Assay**

246 RAW 264.7 macrophages were infected at a 1:1 ratio with STM WT and STM
247 Δ*luxS*. At 16 h, post-infection cells were lysed, and the sample was collected
248 as described above. The competition was also done with the coculture of
249 STM WT and STM Δ*luxS*. This involved the co-cultivation of STM WT and STM
250 Δ*luxS* together, followed by infection in RAW264.7 macrophages. The

251 competitive index was calculated for a WT strain and Δ*luxS* by dividing the
252 ratio between CFU (STM Δ*luxS*) and CFU (STM WT) by the ratio of both strains
253 in the inoculum.

254 **RNA isolation and RT-qPCR**

255 For gene expression study in Luria Bertani (LB) media and F-media (acidic
256 media that mimics the cell vacuole environment) (56) (48), overnight-grown
257 culture in LB media was subjected to subculture (at 1:100) in LB or F-media
258 (**Table S1**). At 3h, 6h,9h, and 12h, bacterial cell pellets were resuspended in
259 TRIzol (from TaKaRa, RNA isoPlus- 9109) and kept at -80˚C. Total RNA was
260 isolated by chloroform extraction followed by isopropanol precipitation. To
261 evaluate the quality, the amount of RNA was quantified in nanodrop
262 (ThermoFischer) and examined on a 2% agarose gel.
263 To produce cDNA, 3 µg of RNA sample was treated with DNase I (TaKaRa)
264 at 37˚C for 1 h followed by heating for 10 min at 65˚C. DNA-free RNA
265 samples were used to make cDNA using the PrimeScript RT reagent Kit
266 provided by TaKaRa (Cat# RR037A).
267 For gene expression in *Salmonella* Typhimurium upon infection in RAW
268 264.7 macrophages, infections were performed at MOI of 20. At 2h, 6h, and
269 16h post-infection, the cells were lysed using TRIzol and kept at -80˚C. Total
270 RNA isolation and cDNA synthesis were carried out using the
271 manufacturer's protocol. The list of expression primers is provided in **Table**
272 **S3**.

273 **Acid survival assay**

274 Overnight cultures of STM WT, STM Δ*luxS,* STM Δ*lsrB,* STM Δ*lsrK,* and STM
275 Δ*lsrR* were adjusted to OD_{600} - 0.3. For survival in 1XPBS, pH was adjusted to
276 3,4,5,6,7, or 8 using concentrated HCl. Strains of *Salmonella* Typhimurium

277 (10^7 bacteria/ml) were exposed to different pH as mentioned in 1X PBS and
278 incubated for 2h. At 2h post-treatment, CFU were enumerated by plating on
279 LB agar media. The same protocol was followed for survival in LB media with
280 similar pH ranges. For the strain of STM harboring plasmids pQE60
281 complemented with *phoP*/*phoQ*, a survival assay was done in pH of 3, 4, and
282 5 in 1X PBS.

283 **Acid tolerance assay**

284 A standard acid tolerance assay was performed as previously described with
285 slight modification (22). Briefly, acid tolerance assay (ATR) was conducted
286 with strains grown overnight at 37°C in LB broth containing the appropriate
287 antibiotic. The culture corresponding to 0.3 OD_{600} of the overnight culture
288 (unadapted) was centrifuged and the pellet was resuspended into 2 ml of LB
289 broth (pH 5) and incubated at 37°C with shaking for 2 h (known as adapted
290 culture). The acid challenge of unadapted and adapted cultures involved
291 readjusting the pH to 3. CFU was determined for adapted and unadapted
292 cultures after exposure to pH 3 (2 h of pH 3 treatment). ATR assay was also
293 done with the strain of *Salmonella* containing plasmid pQE60
294 complemented with *phoP/phoQ* gene.

295 **Intracellular pH measurement by pHuji plasmid**

296 The plasmid pBAD:pHuji (Plasmid #61555) was used to transform STM WT,
297 STM Δ*luxS*, STM Δ*lsrB*, STM Δ*lsrK*, and STM Δ*lsrR*. pHuji is a pH-sensitive red
298 fluorescent protein demonstrating a more than 20-fold fluorescent intensity
299 change from pH 5.5 to 7.5 (57). Overnight-grown bacterial strains were
300 subjected to a pH range of 3.0 to 8.0 in phosphate buffer (PBS) in 40μM of
301 sodium benzoate to ensure equilibration to the desired pH. The resulting
302 fluorescence intensity ratio, obtained from flow cytometric analysis, was

303 plotted as a function of pH and fitted to get a standard curve. The standard
304 curve was used to interpolate ratios measured within the intracellular pH of
305 bacteria in LB media, F-media, and RAW 264.7 macrophages.

306 **Mass-spectrometry for the determination of lysine and cadaverine**

307 Overnight grown STM WT, STM Δ*luxS*, STM Δ*lsrK,* STM Δ*lsrB,* and STM Δ*lsrR*
308 were sub-cultured in acidic pH 5 LB media and incubated at 37℃ until mid-
309 log phase. Thereafter, bacteria were spun down and the spent media were
310 collected. Spent media were kept with an equal volume of acetone at -20℃
311 for overnight. Next, samples were collected after centrifugation at 13k rpm
312 for 10 min. Samples were analysed in Orbitrap fusion connected to UHPLC
313 Vanquish (Thermo Scientific). Water and acetonitrile with 0.1% formic acid
314 were used as a mobile phase. The flow rate was kept at 0.3ml/min linear
315 gradient was started with 5% to 95% using Hypersil Gold C18 column
316 (2.1X100mm & particle size 1.9µ).

317 **Plasmid construction, and site-directed mutagenesis**

318 The vector pET28a(+) was used to construct plasmids p*lsrR* for the
319 overexpression of LsrR as a C-terminal 6xHis-tagged fusion protein. The
320 DNA fragment containing *the lsrR* coding region was amplified by
321 polymerase chain reaction (PCR) from the chromosome of *Salmonella*
322 Typhimurium 14028s using primers (F-lsrR and R-lsrR containing restriction
323 site NcoI and XhoI, respectively). The PCR products were digested with NcoI
324 and XhoI, and ligated with NcoI and XhoI digested pET28a(+). The inserts
325 were checked by DNA sequencing.

326 For Y25A and R43A site-directed mutagenesis in LsrR protein, PCR for SDM
327 was set up with template DNA from pETa(+)- *lsrR* and amplified with Q5
328 polymerase (NEB). The PCR products were digested with DpnI and

329 transformed into *E. coli* DH5-alpha. Y25A and R43A double mutants were
330 generated using pET28a(+) *lsrR* R43A plasmid as a template for SDM using
331 primers specific to the second set of mutations. All plasmids were
332 confirmed by DNA sequencing.

333 **Overexpression, and purification of LsrR**

334 pET28a(+)-*lsrR* and its mutants containing C-terminal 6xHis tag were
335 transformed into *E. coli* Rosetta (DE3). The transformed colonies were
336 inoculated into 5 ml LB containing kanamycin (Kan) and chloramphenicol
337 (Cm) and grown overnight. Inoculum (1%) was added to 1.2 L LB containing
338 Kan and Cm, grown at 37°C to an OD_{600} of 0.4 under shaking, and thereafter
339 supplemented with 0.1 mM IPTG, and grown at 16℃ overnight. Cells were
340 harvested by centrifugation at 4℃, resuspended in 10 ml buffer A [20 mM
341 Tris–HCl pH 8, M NaCl, 10% glycerol (v/v), 1.5 mM β-mercaptoethanol, 1 mM
342 PMSF] lysed by sonication, and centrifuged at 4℃ in a pre-cooled centrifuge
343 at 10000 rpm for 10 min. The supernatant was loaded onto a 1 ml Ni-NTA
344 column equilibrated with buffer A, washed with 20 ml buffer A, and eluted
345 with a gradient of imidazole (20–500 mM) in the same buffer. The fractions
346 were analysed on 12% SDS-PAGE. Fractions enriched for LsrR were pooled,
347 loaded onto a Superdex75 gel filtration column, and eluted in buffer B [20
348 mM Tris–HCl pH 8, 1M NaCl, 10% glycerol (v/v) and 1.5 mM β-
349 mercaptoethanol]. The purity of LsrR was checked on 12% SDS-PAGE **(Fig.
350 S7H)**. Fractions with apparent homogeneity were pooled, concentrated
351 using a 10 kDa cut-off Centricon (Millipore), and estimated by Bradford's
352 method using bovine serum albumin (BSA) as standard. The proteins were
353 dialyzed against buffer A containing 50% glycerol (v/v) and stored at –20˚C.

354 **Gel shift assay**

355 HPLC-purified 90bp single-strand DNA oligos of the *lsrR* and *phoP* operon
356 promoters (Sigma) were used for a gel shift assay. Binding reactions involved
357 incubating promoter DNA with varying concentrations of LsrR or its mutated
358 form. The incubation buffer contained 50 mM Tris-Cl (pH 7.5), 150 mM NaCl,
359 3 mM magnesium acetate, 0.1 mM EDTA, and 0.1 mM DTT. After 15 min at
360 room temperature, the mixture was combined with gel loading buffer (60%
361 0.25× TBE, 40% glycerol, 0.2% bromophenol blue) and run on a 6% native
362 polyacrylamide gel. The staining was done for DNA with SYBR™ Gold Nucleic
363 Acid Gel Stain (Invitrogen) and analyzed as per the manufacturer's
364 instructions.

365 ***In vivo* animal experiment**

366 Oral gavaging of 10^7 CFU of STM WT, STM*ΔluxS*, STM*ΔlsrB*, STM*ΔlsrK*,
367 STM*ΔlsrR*, and STM*ΔluxS:luxS* was used to infect 5- to 6-week-old C57BL/6J
368 mice. Post five days of infection, the intestine (Peyer's patches), MLN
369 (mesenteric lymph node), spleen, liver, and blood were aseptically
370 extracted (in a Biosafety level 2 cabinet) to examine the colonization in the
371 organs. The CFU were enumerated on differential and selective *Salmonella-*
372 *Shigella* (SS) agar.

373 **Mice survival assay**

374 Male C57BL/6, aged 5 to 6 weeks, were obtained from the Central Animal
375 Facility, IISc. The mice were given 10^8 CFU of each strain (overnight grown
376 cultures) orally to compare the survival and weight alterations of mice post-
377 infection. Following infection, the mice were observed every day to
378 determine their survival and weight, and the results were expressed as a
379 percentage of survival (Kaplan-meier curve) and weight reduction.

All experiments comply with the rules set forth by the Indian Institute of Science, Bangalore's IEAC. The approved protocol number is CAF/ Ethics/852/2021. The Institutional Animal Ethics Committee approved every animal experiment, and the National Animal Care Guidelines were scrupulously followed.

Statistical analysis

As mentioned in figure legends, each experiment has been independently repeated two to five times. GraphPad Prism 8.4.3 was utilized for all statistical analyses. As the figure legends state, the statistical analyses included an unpaired, two-tailed Student's t-test, One-way ANOVA with Dunnet's post hoc test, and Two-way ANOVA with Tukey's post hoc test. A non-parametric one-way ANOVA (Kruskal Wallis) test with Dunn's post-hoc test was performed for the animal experiment. P-values less than 0.05 were regarded as significant. The analysis is presented as mean ±SD or mean ±SEM with information on group sizes and p values mentioned in the respective figure legends.

397 **Results**

398 **LuxS/AI-2 quorum sensing is required by *Salmonella* Typhimurium to**
399 **survive in the macrophages**

400 We first investigated the levels of AI-2 produced at different growth phases
401 from *Salmonella* Typhimurium (STM) WT grown at 37℃ in LB media by using
402 the *Vibrio harveyi* BB-170 reporter strain (which produces luminescence
403 responses to AI-2). Consistent with previous studies (16), AI-2 dependent
404 light production by *V. harveyi* BB-170 is maximum in the spent medium of
405 the mid-log phase culture of STM, and it gradually decreases towards the
406 late stationary phase **(Fig. 1A; Fig. S1A)**. Also, while *Salmonella* upregulated
407 the expression of the *lsr* operon genes (*lsrB*, *lsrK*, *lsrR*) during its mid-log
408 phase to early stationary phase of growth **(Fig. 1B)**, it did not alter the
409 expression of *luxS* during this period **(Fig. 1C)**. And the deletion of *luxS* and
410 *lsr* operon genes (*lsrK*, *lsrB*, *lsrR*) in STM did not affect the *in vitro* growth in
411 LB and minimal media **(Fig. S1B, C)**. Next, we observed that in comparison
412 to the STM WT, the quorum-sensing mutants STM*ΔluxS*, STM*ΔlsrB*, and
413 STM*ΔlsrK* displayed increased phagocytosis in RAW 264.7 macrophages
414 **(Fig.1D)**. However, both STM*ΔlsrR*, and *luxS* complemented STM*ΔluxS*
415 behaved same as STM WT **(Fig.1D)**. Importantly, the STM*ΔluxS*, STM*ΔlsrB*,
416 and STM*ΔlsrK* but not the STM*ΔlsrR*, and *luxS* complemented STM*ΔluxS*
417 showed a decreased ability to proliferate in RAW 264.7 cells **(Fig .1E; Fig.**
418 **S1E, F)**.

419 Further, we noted that the *luxS* and the *lsrB*, *lsrK,* and *lsrR* genes showed
420 1.5–2 fold upregulation post 6h of infection into RAW 264.7 macrophages till
421 16h **(Fig. 1F, G**). We further corroborated our results by using primary
422 macrophages derived from the peritoneal lavage of C57BL/6J mice for

423 infection. The *luxS, lsrB*, and *lsrK* mutants also exhibited an increased
424 uptake by the primary macrophages, but their proliferation was
425 compromised **(Fig. 1H, I)**. Furthermore, we checked for AI-2 production by
426 STM WT, STMΔ*luxS*, and STMΔ*lsrB* upon their infection of RAW 264.7 cells
427 and observed the AI-2 production by STM WT and STMΔ*lsrB* till 16h post-
428 infection but not by STMΔ*luxS* **(Fig. S1D)**. Taken together, these findings
429 imply that *Salmonella* Typhimurium requires LuxS/AI-2 signaling to survive
430 in the hostile environment of macrophages.

431 **STM Δ*luxS* acquires AI-2 from STM WT during its *in vitro* growth but may**
432 **not do so within its intravacuolar niche**

433 To find out if STMΔ*luxS* can use AI-2 molecules produced by STM WT, we co-
434 infected RAW 264.7 macrophages with STM WT and STMΔ*luxS* (1:1 ratio),
435 and observed that STM WT outcompeted STMΔ*luxS,* hinting that STMΔ*luxS*
436 may not be able to utilize the AI-2 from STM WT within host macrophages.
437 **(Fig. 2A)**. However, when STM WT and STMΔ*luxS* were cocultured in LB
438 media before infection into macrophages, STM WT and STMΔ*luxS*
439 proliferated similarly in RAW 264.7 cells **(Fig. 2B)**. To check if STMΔ*luxS* can
440 utilize AI-2 molecule produced by STM WT, we treated STMΔ*luxS* with the
441 STM WT spent media and exogenous DPD molecule. Upon infection into
442 RAW 264.7 macrophages, the treated STMΔ*luxS* proliferated similarly to
443 STM WT, suggesting its ability to use the AI-2 from the spent media of STM
444 WT or exogenous DPD **(Fig. 2C, D; Fig. S2A-D).** Next, we used a
445 commercially available inhibitor (Z)-4- bromo-5-(bromomethyllene)-3-
446 methylfran-2(5H) (BF-8) of LuxS/AI-2 signaling (18) (19) at different
447 concentrations with STM WT and observed that while BF-8 did not affect
448 STM WT growth *in vitro*, it attenuated its survival in RAW 264.7 macrophages
449 similar to that observed with STMΔ*luxS* **(Fig. 2E, F; Fig. S2E)**. We also

450 confirmed the light production and inhibition upon synthetic DPD and
451 inhibitor BF-8 treatments by autoinducer assay **(Fig. S2F, G).** Infections into
452 the peritoneal macrophages suggested that while exogenous DPD
453 enhanced STMΔ*luxS* survival, BF-8 attenuated the STM WT proliferation **(Fig.**
454 **S2H, I).** These findings imply that the *luxS* mutant can utilize exogenous AI-
455 2 during its *in vitro* growth but not within its intravacuolar niche.

456 **The loss of a functional AI-2 or its receptor-mediated sensing attenuates**
457 ***Salmonella* survival at acidic pH**

458 Quorum sensing pathways monitor changes in the density of the bacterial
459 population and control the expression of genes involved in critical cellular
460 processes, such as survival and pathogenicity (20). The mechanisms
461 underlying bacterial quorum sensing and pH sensing have been thoroughly
462 investigated and shown to be distinct/independent gene regulatory
463 systems. Our study shows that environmental acidification is the critical
464 physiological signal that upregulates AI-2 production by *Salmonella* **(Fig.**
465 **2G).** Hence, we hypothesize that LuxS/AI-2 signaling may coordinate with the
466 pH sensing system of *Salmonella* to regulate survival in an acidic
467 environment. Firstly, when we assessed the expression of mRNAs from *luxS*
468 and *lsr* operon during its growth in F-media (mimics the acidic vacuolar
469 condition), we observed ~1.5-fold increases in *luxS* at the mid-log phase to
470 the late-log phase **(Fig. S3A),** and *lsrB*, *lsrK,* and *lsrR* at the mid-log phase
471 **(Fig. S3B)**. Moreover, we observed that STM stably produces AI-2 even during
472 its growth in F-media (at pH 5), which is maximal during the mid to late-log
473 phase **(Fig. 2G).** The luminescence production continued in STM*ΔlsrB* spent
474 media even beyond 12 h (because there was no accumulation of AI-2 inside
475 the STM *ΔlsrB*). However, there was no light production from the spent
476 medium of STM*ΔluxS* **(Fig. 2G)**.

477 To underscore the role of AI-2 in facilitating survival in an acidic
478 environment, we performed an acid survival assay and noted that STM WT,
479 STM*ΔluxS*, ST *ΔlsrB*, STM*ΔlsrK*, and STM*ΔlsrR* survived equally well at pH6 to
480 pH8 **(Fig. S3C)**. However, at pH3, pH4, and pH5, STM WT survived
481 significantly better **(Fig. 2H-J; Fig. S3D-G)**. We conclude that LuxS/AI-2
482 signaling and communication facilitate *Salmonella's* survival strategies in
483 acidic environments under *in vitro* conditions.

484 **LuxS/AI-2 system tunes *phoP/phoQ* expression, thereby assisting in pH**
485 **sensing and adaptation in *Salmonella***

486 Jesudhasan et al., 2010 determined that there is a differential gene
487 expression between the STM WT and STMΔ*luxS* (21) pertaining to virulence,
488 flagellar, and motility genes. A well-known two-component system(TCS) of
489 PhoP/PhoQ is essential in mediating the acid tolerance response (ATR) in
490 several Gram-negative bacteria, including *Salmonella* (22) (23). Thus, we
491 conjectured that LuxS/AI-2 signaling modulates the *phoP/phoQ* gene
492 expression, which, in turn, aids in the survival of *Salmonella* under an acidic
493 environment. Thus, we questioned if phosphorylation of AI-2 is essential to
494 regulate the expression of the downstream gene targets apart from the *lsr*
495 operon **(Fig. 3A)**.

496 We observed that compared to STM WT, mRNA expression of *phoP* is
497 downregulated in STM*ΔluxS*, STM*ΔlsrB*, and STM*ΔlsrK* in LB **(Fig. 3B; Fig.**
498 **S4A)** and F-media **(S4B, D)**. Interestingly, the *phoP* expression was rescued
499 when STM*ΔluxS* was grown in STM WT spent media **(Fig. 3C)**. Additionally,
500 upon infection in macrophages, both *phoP* and *phoQ* were under-expressed
501 in the mutants compared to STM WT **(Fig. 3D, E; Fig. S4C)**. Hence, we
502 conclude that AI-2 sensing and the signaling cascade orchestrate the
503 *phoP/phoQ* expression in *Salmonella* Typhimurium.

504 Next, we evaluated the ATR and noted that with a prior adaptation to pH 5,
505 only STM WT and STM*ΔlsrR* were resilient and showed better survival upon
506 exposure to pH 3 **(Fig. 3F)**. As the STM*ΔluxS*, STM*ΔlsrB*, and STM*ΔlsrK*
507 exhibited a diminished ATR, we determined the intracellular pH of all the
508 strains using a pH-sensitive pHuji plasmid. We observed that all the
509 *Salmonella* strains maintained their cytosolic pH in the neutral LB media
510 (pH 7). However, when grown in acidic F-media (pH 5), STM WT and
511 STM*ΔlsrR* could maintain their cytosolic pH within the near-neutral range
512 while cytosolic pH for STM*ΔluxS*, STM*ΔlsrB*, and STM*ΔlsrK* dropped to pH
513 5.1, 5.2, and 5.0, respectively and to 5.6, 5.4, and 5.2 (±0.2) respectively
514 within the hostile macrophages **(Fig. 3G; Fig. S4E-I).**
515 The PhoP/PhoQ TCS aids in pH homeostasis via the *cadC/BA* system
516 (transcriptional regulator, lysine/cadaverine antiporter and lysine
517 decarboxylase), thereby promoting bacterial survival in mildly acidic
518 environments (24, 25). The diminished mRNA expression of *cadC*, *cadB*, and
519 *cadA* in STMΔ*phoP* upon infection in RAW 264.7 macrophages validated the
520 above observation **(Fig. S5A-C)**. The lysine decarboxylase (CadA) quenches
521 the H^+ while converting lysine to cadaverine, which is exported to the
522 extracellular milieu by CadB (24). Here, we noted the cadaverine/lysine
523 ratio to be low in STM*ΔluxS*, STM*ΔlsrB*, and STM*ΔlsrK* compared to STM WT
524 under an acidic pH of 5 **(Fig. 3H).** Additionally, in the mutants, the *cadA*,
525 *cadB*, and *cadC* genes were under-expressed at 2h, 6h, and 16h post-
526 infection into RAW 264.7 cells **(Fig. 3J, K, L).** From a mechanistic
527 perspective, we conclude that LuxS/AI-2 signaling regulates ATR and
528 maintains the cytosolic pH of *Salmonella* by regulating *cadC/AB* operon via
529 *phoP/phoQ*.

530 **LuxS/AI-2 signaling regulates *phoP/phoQ* expression through LsrR**
531 **interaction with the *phoP* promoter in *Salmonella***
532 We explored whether LsrR, the downstream regulator of the LuxS/AI-2
533 signaling pathway, could directly interact with the *phoP* promoter to
534 influence its activity. The AlphaFold3 structure revealed that LsrR binds to
535 both the DNA strands of the *lsr* promoter, but to only one of the strands of
536 the *phoP* promoter (26). The interactions are mediated by residues Y25, T31,
537 Q32, S33, R43, L44, K45, S47, and R48, all within a distance of <5 Å and a
538 predicted aligned error (PAE) of <14 across multiple replicates **(Fig. 4A, B;**
539 **Fig. S6A, B)**. These residues are located in the N-terminal domain, spanning
540 positions 25-48, between alpha helices 1, 2, and 3. Notably, Y25, T31, and
541 R43 contributed the most significant interactions, with R43 from helix 3
542 displaying the highest number of contact points (27). A covariance analysis
543 of the multiple sequence alignment revealed that R43 most frequently co-
544 occurs with Y25, an interacting residue located in helix 1, with the highest
545 probability among all analyzed residues (28). Given the strong interactions
546 of R43 and Y25 with the *lsr* and *phoP* promoters, we generated Y25A, R43A,
547 and Y25A/R43A mutants and used AlphaFold3 to predict structural impacts.
548 The AlphaFold structures indicated that the mutations severely disrupted
549 promoter interactions, with PAE values exceeding 18 and pLDDT scores for
550 all the DNA-contacting residues dropping below 30. Additionally, we
551 performed NPT ensemble molecular dynamics simulations for the mutant
552 protein-DNA complex, which revealed a significant weakening of
553 interactions. We validated our findings *in vitro* through electrophoretic
554 mobility shift assays (EMSA) using purified wild-type LsrR and its Y25A,
555 R43A, and Y25A/R43A mutants to assess their binding to HPLC-purified *lsr*
556 and *phoP* promoters **(Fig. 4D, E; Fig. S6C-F)**. WT LsrR bound both

557 promoters, Y25A showed reduced binding, R43A further reduced it, and the
558 double mutant lost nearly all binding at 200mM NaCl **(Fig. S7A, B)**. A similar
559 result was observed for the interaction of LsrR with a single-stranded
560 promoter sequence **(Fig. S7C-F),** and a random DNA sequence did not show
561 any interaction (**Fig. S7G)**. To assess regulatory effects during infection, we
562 generated a *luxS/lsrR* double knockout and complemented it with *lsrR* (WT)
563 and mutant *lsrR*. While the double knockout strain proliferated similarly to
564 WT STM, *lsrR* complementation reduced proliferation. The Y25A/R43A
565 mutant restored survival to knockout levels **(Fig. 4E, F)**, indicating LsrR's
566 binding to *lsr* and *phoP* promoters acts as a negative regulator of *Salmonella*
567 pathogenicity.

568 **AI-2 orchestrates the *Salmonella* Pathogenicity Island-2 gene**
569 **expression by sensing low pH**

570 PhoP has been shown to control the TCS SsrA/SsrB at the transcription level,
571 which are the master regulators of the SPI-2 genes (29). The expression of
572 *ssrA* and *ssrB* genes was also downregulated in STMΔ*phoP* upon infection
573 into RAW 264.7 cells **(Fig. S8A, B)**. Thus, we hypothesized that LuxS/AI-2
574 signaling might control the SsrB/SsrA system via PhoP/PhoQ. Upon infection
575 into RAW 264.7 macrophages, the mRNA expression of *ssrB* was
576 downregulated from early stage post-infection to late stage post-infection in
577 macrophages **(Fig. 5A)**. On the other hand, *ssrA* was downregulated at a late
578 stage post-infection **(Fig. 5B)**. Furthermore, we observed expression of *ssaV*
579 a Type 3 secretion system (T3SS) needle complex protein, encoded by SPI-2
580 and *spiC* an SPI-2 encoded effector molecule were under-expressed in the
581 absence of *luxS, lsrB,* and *lsrK* genes in STM upon infection into RAW 264.7
582 macrophages **(Fig. 5C, D).**

583 So far, our findings convey that the LuxS/AI-2 signaling regulates *phoP/phoQ*
584 genes and, thereby, the SPI-2 cluster in *Salmonella*. However, whether AI-2
585 directly or the AI-2-PhoP/PhoQ axis controls the SPI-2 genes remains
586 unclear. Thus, we cloned the *phoP/phoQ* operon under a non-native
587 promoter in the pQE60. We confirmed the *phoP* mRNA overexpression level
588 in STM WT:pQE60-*phoP/phoQ* and STM*ΔluxS:*pQE60-*phoP/phoQ* upon
589 infection in RAW 264.7 **(Fig. S8C, D)**. Using these complemented
590 *Salmonella* strains, we observed that STM*ΔluxS*, STM*ΔlsrB*, and STM*ΔlsrK*
591 with a *phoP/phoQ* cloned under a non-native promoter survived equally at
592 acidic pH3, 4, and 5 as STM WT **(Fig. 5E-G)**. Furthermore, the STM*ΔluxS*,
593 STM*ΔlsrB*, and STM*ΔlsrK* with cloned *phoP/phoQ* showed enhanced ATR
594 response **(Fig. 5H)**. Thus, when *phoP/phoQ* is not under its native promoter,
595 the regulation by LuxS/AI-2 is not required. Also, *ssrB* and *ssrA* expression
596 are significantly higher in *phoP/phoQ* complemented knockout strains
597 compared to STM*ΔluxS*, STM*ΔlsrB*, and STM*ΔlsrK* strains **(Fig. 5I-K; Fig. S8E-**
598 **G)**. Cumulatively, these results suggest that, indeed, the LuxS/AI-2
599 signalling controls ATR by regulating the *phoP/phoQ* genes.

600 **The absence of AI-2 mediated signaling compromises the *in vivo***
601 **colonization of *Salmonella* in mice**

602 The gastrointestinal tract is a diverse and dynamic environment in which
603 bacterial species communicate with each other to coordinate the
604 expression of various genes (30). While many quorum sensing signals are
605 species-specific, AI-2 signalling is known as universal quorum sensing
606 signaling. Because AI-2 produced by one species can affect the expression
607 of genes in another, this signal can promote communication across species
608 and allow bacteria to alter behaviors like pathogenicity, and the production
609 of biofilms among various species (31). Because of this characteristic, AI-2

610 is an excellent choice to mediate interactions between cells in the
611 mammalian gut, where hundreds of bacterial species live and interact. It
612 has already been determined that several gut-associated bacteria encode
613 LuxS (the AI-2 synthase) or generate AI-2 (32). Of the major families
614 dominating the gut consortium, more than 80% of Firmicutes have been
615 detected to encode the LuxS enzyme (33). While members of the families
616 *Barnesiellaceae* and *Muribaculaceae* are predominant producers of AI-2 in
617 the gut (34). Thus, we aimed to understand the role of LuxS/AI-2 signalling in
618 regulating *Salmonella* pathogenesis in *in vivo* mice models.
619 We infected C57BL/6J mice by orally gavaging with STM WT and knockout
620 strains at a CFU of 10^7 per mouse **(Fig. 6A**). We observed that STM*ΔluxS*,
621 STM*ΔlsrB*, and STM*ΔlsrK* showed a significantly lower organ burden in the
622 intestine, MLN, spleen, and liver and lower bacteraemia upon oral gavage
623 **(Fig. 6B–F)**. Oral gavage mimics the physiological route of *Salmonella*
624 infection into its host, and *Salmonella* is required to be able to breach the
625 intestinal barrier successfully. The lower organ colonization in STM*ΔluxS*,
626 STM*ΔlsrB*, and STM*ΔlsrK* can be explained by their inability to cross the gut
627 epithelial barrier. Next, we bypassed the gut epithelial barrier by infecting
628 C57BL/6 mice intraperitoneally and found that STM*ΔluxS,* STM*ΔlsrB, and*
629 STM*ΔlsrK* still exhibited reduced colonization in the spleen and liver and less
630 dissemination in blood than STM WT **(Fig. S9A-D).** Furthermore, upon
631 infection of mice by oral gavaging at a CFU of 10^8 per mouse, we noted that
632 the mice infected with STM WT and STM*ΔlsrR* succumbed to death as early
633 as the 6th day of post-infection, while STM*ΔluxS*, STM*ΔlsrB*, and STM*ΔlsrK*
634 infected mice survived longer **(Fig. 6G-H)** with less weight reduction **(Fig.**
635 **S9E)**. Further, we observed that the BF-8 inhibitor at 4 mg/kg reduced the
636 STM WT colonization to different sites of infection in C57BL/6 mice **(Fig. 6I-**

637 **N**) and improved the survival of mice with delayed weight reduction
638 compared to untreated mice **(Fig. 6O, P; Fig. S9F).** Liver tissue
639 histopathology results also suggest that treatment with BF-8 reduced the
640 disease score **(Fig. S9G)**. Our results show that LuxS/AI-2 signaling is critical
641 for the *in vivo* pathogenesis and virulence of *Salmonella* Typhimurium.

642 **Discussion**

643 The human body serves as a host for a vast array of microorganisms
644 collectively known as the normal microbiota. These microbes coexist
645 closely with their host and often offer significant health benefits, especially
646 within the intestine. These microbes supplement our metabolism by
647 producing essential vitamins like B and K, generating vital compounds such
648 as short-chain fatty acids (SCFAs). These microbial functions play a key role
649 in maintaining intestinal homeostasis, protecting and defending against
650 both gut and systemic infections(35, 36).

651 Understanding how these microbial interactions influence health is critical,
652 especially given the rising prevalence of infectious and chronic diseases
653 linked to disruptions in the microbiota, also known as dysbiosis. One major
654 trigger of dysbiosis is the use of broad-spectrum antibiotics and the use of
655 secondary metabolites or chemical signals by pathogens, which can
656 drastically alter the composition and diversity of gut bacteria(37, 38). These
657 changes often reduce beneficial taxa while allowing harmful ones to
658 proliferate. This illustrates the principle of colonization of a pathogen to
659 establish an infection. This is true in the case of the enteric pathogen
660 *Salmonella*. In the Oligo-mouse-microbiota (OMM^{12}) model of infection,
661 *Salmonella* induces compositional changes in the synthetic consortium
662 (39). A previous study showed that the OMM^{12} mice model provides less

colonisation resistance to *Salmonella* infection (40). It can be perceived that the ability of this pathogen to cause microbial shifts via distinct mechanisms is a stealthy trategy to evade colonisation resistance in the gut.

Beyond metabolism, behaviors such as motility, surface adherence, and biofilm formation further shape microbial dynamics. These processes are often coordinated through quorum sensing a communication system where bacteria release chemical signals called autoinducers to monitor population density and regulate gene expression collectively(20). Given the multispecies nature of this environment, cross-species signaling likely enables microbes to fine-tune their behaviors in response to social and environmental cues. Studies show that AI-2 facilitates interspecies communication and modulates behavior across species lines, leading to the hypothesis that AI-2 plays a central role in regulating microbial interactions and community dynamics in the gut(41).

The aspects of the bacterial lifestyle and pathogenesis rely on the bacterial quorum and community attributes, like for *Salmonella*, the infectious dose to cause the illness in humans is more than 10,000 CFU(42). Autoinducers are chemical signal molecules that underpin bacterial communication and differ amongst species, just like the different languages that exist across the human civilization. Here, we report that as a successful enteric pathogen, *Salmonella* can use the AI-2 molecule to coordinate and break the colonization resistance in the gut. AI-2 synthesis and *lsr* operon are concurrently regulated under neutral and acidic conditions in *Salmonella,* aiding in its survival. The phosphorylation of AI-2 by LsrK is crucial for its function (43) and is validated by our study, where we observe that deletion

688 of *lsrK* renders *Salmonella* incapable of surviving in macrophages and
689 incapable of upregulating *phoP* expression.

690 The gastrointestinal tract presents with a dynamic environment where
691 microbes compete for space and nutrients through various mechanisms.
692 Many gut-associated bacteria encode LuxS or produce AI-2, including a
693 significant proportion of Firmicutes and Proteobacteria, and some species
694 of Bacteroidetes and Actinobacteria (38). *Salmonella* might benefit from the
695 AI-2 produced by the gut commensals in the intestinal lumen. Our *in vivo*
696 studies justify it to some extent with compromised colonization of the
697 primary and secondary sites of infection upon abrogation of LuxS/AI-2
698 signaling in *Salmonella*. Although the neighboring bacteria might produce
699 AI-2 in the intestinal niche, STMΔ*lsrB* and STMΔ*lsrK* cannot utilize AI-2 to
700 mediate the downstream signaling cascades. Thus, we underscore the
701 critical function of individual members of this cascade, the AI-2 synthesizing
702 enzyme, receptor, and kinase enzyme. Our study of baceterial strain co-
703 culture prior to infection further suggests the ability of *Salmonella* to utilise
704 the microbiota produced AI-2 molecules in the gut.
705 During intestinal colonization, a prime strategy of this pathogen is to activate
706 the ATR systems to endure the harsh environment. The four major regulators
707 that control relevant stress responses in *Salmonella* are RpoS, PhoPQ, Fur,
708 and OmpR/EnvZ (44). We describe a mechanism that AI-2 signaling tunes
709 the expression of the two-component system *phoP/Q*, which helps in ATR.
710 Relating to intravacuolar survival, studies show that the acidic pH of the
711 vacuole is necessary for the assembly of T3SS encoded by SPI-2, but not for
712 the effector molecule's secretion (45). Yet, it is essential to maintain the
713 neutral pH of the bacterial cytoplasm to secrete the effector molecule,
714 which we found to be lost upon abrogation of AI-2 signaling (46). Thus,

715 *Salmonella* regulates its cytosolic pH in acidic environments via the AI-2
716 signaling and tries to sustain its intracellular pH near neutral to maintain the
717 regular cellular functions and secretion of SPI-2 effectors for its survival and
718 proliferation within the macrophages. Moreover, *Salmonella* AI-2
719 phosphorylation by LsrK is a key process in controlling the downstream
720 targets. While our study elucidates the mechanism of acid tolerance and
721 macrophage survival via AI-2 signaling in *Salmonella*, it has some
722 limitations. We cannot conclusively determine whether STMΔ*luxS* utilizes
723 AI-2 from STM WT in the coinfection study in RAW 264.7 cells **(Fig. 2A)**.
724 Furthermore, the study does not confirm whether both bacterial strains
725 infect the same cell, as observations reflect a global phenotype. However, it
726 might be possible that STM *ΔluxS* cannot utilize AI-2 even when infecting the
727 same cell due to a repressed *lsr* operon.
728 We broaden the horizon of LsrR regulation of gene expression beyond the *lsr*
729 operon by unraveling the binding of LsrR to the *phoP* promoter via its Y25 and
730 R43. Interestingly, these insights also shed light on an unusual interaction
731 of the LsrR with a single strand of the DNA at the promoter site. This not only
732 identifies the mechanism but also paves the way to a "secret garden" of
733 genes that may be regulated by LsrR. While this observation is in
734 *Salmonella,* it can be extrapolated to other bacteria that utilise a similar AI-
735 2 signalling cascade. Overall, we identify a regulatory network via AI-2 and
736 PhoP/PhoQ TCS, leading to a remarkable survival strategy for *Salmonella*
737 under acidic pH. A proposed strategy for controlling *Salmonella* infections
738 focuses not on bactericidal activity, as in the case of conventional
739 antimicrobials, but rather on disrupting a key functional process critical to
740 the pathogen's infectious lifecycle. One promising target is the
741 communication, wherein *Salmonella* uses it to actively survive in the acidic

environment of the stomach, colonizes in the intestine, followed by a secondary site of infection, and survives in the hostile niche of macrophages, which is an essential step for successful pathogenesis. These virulence process depends on the coordinated regulation of numerous virulence genes, which are modulated through an intricate network of genetic and environmental signals. Our *in-vivo* study suggests that inhibition of LuxS/AI-2 signaling attenuates *Salmonella* colonization. Our findings highlight and open promising avenues to target the bacterial communication and AI-2 signaling, for designing antibacterial strategies to limit *Salmonella* infection.

Funding

This work was funded by the Department of Biotechnology (DBT), Ministry of Science and Technology, the Department of Science and Technology (DST), Ministry of Science and Technology. DC acknowledges DAE-SRC (DAE00195) outstanding investigator award and funds and ASTRA Chair Professorship funds. The authors jointly acknowledge the DBT-IISc partnership program. Infrastructure support from ICMR (Center for Advanced Study in Molecular Medicine), DST (FIST), UGC-CAS (special assistance), and TATA fellowship is acknowledged. AS duly acknowledges UGC-SRF for the financial assistance. AVN duly acknowledges the IISc-MHRD for the financial assistance. SA duly acknowledges the CSIR for the financial assistance. SD and SK with SM duly acknowledge IISc Bangalore for their financial support. RSR acknowledges IISc for the financial help.

Ethics statement

All experiments comply with the rules set forth by the Indian Institute of Science, Bangalore's IEAC. The approved protocol number is CAF/ Ethics/852/2021. The Committee for Control and Supervision of Experiments on Animals (CPCSEA), a statutory committee established under Chapter 4, Section 15 (1) of the Prevention of Cruelty to Animals Act 1960, and National Animal Care provided guidelines that were meticulously adhered to during all animal experiments, all of which were approved by the Institutional Animal Ethics Committee. (Registration No. 435 48/1999/ CPCSEA). The Institutional Animal Ethics Committee approved every animal experiment, and the National Animal Care Guidelines were meticulously followed.

Author contributions

AS and DC conceived the study. AS and DC designed experiments. AS and AVN performed experiments. SA conducted structural analysis, and AS and SA performed interaction studies under the supervision of UV. SM supervised the synthetic DPD molecule synthesis. SD and SK synthesized the synthetic DPD molecule. RSR analyzed the tissue histopathology. AS analyzed the data, prepared the figures, and wrote the manuscript draft. AS, AVN, SA, SM, UV, and DC reviewed and edited the manuscript. DC supervised the work. All the authors read and approved the manuscript.

Disclosure statement

The authors declare no conflict of interest.

Acknowledgment

Dr. Shashank Tripathi (CIDR, IISc Bangalore) and Dr. Sandeep M Eswarappa (Dept. of Biochemistry, IISc Bangalore) are duly acknowledged for the

Luminometer. Divisional Mass Spectrometry facility IISc and Mrs. Sunita Joshi for the MS analysis. The Departmental Confocal Facility, Departmental Real-Time PCR Facility, Divisional Flowcytometry Facility, and Central Animal Facility at IISc are duly acknowledged. Mr Sumith and Ms Navya are acknowledged for their help in image acquisition. Dr. Ritika Chatterjee and Ms. Sagrika are acknowledged for technical help. Schematic images were created with BioRender (BioRender.com).

Data availability statement

The data that support the findings of this study are available from the corresponding author (DC) upon request.

References-

1. Ehuwa O, Jaiswal AK, Jaiswal S. Salmonella, Food Safety and Food Handling Practices. Foods. 2021;10(5).
2. Eswarappa SM, Negi VD, Chakraborty S, Chandrasekhar Sagar B, Chakravortty D. Division of the Salmonella-containing vacuole and depletion of acidic lysosomes in Salmonella-infected host cells are novel strategies of Salmonella enterica to avoid lysosomes. Infection and immunity. 2010;78(1):68-79.
3. Drecktrah D, Knodler LA, Ireland R, Steele-Mortimer O. The mechanism of Salmonella entry determines the vacuolar environment and intracellular gene expression. Traffic. 2006;7(1):39-51.
4. Holden DW. Trafficking of the Salmonella vacuole in macrophages. Traffic. 2002;3(3):161-9.
5. Haraga A, Ohlson MB, Miller SI. Salmonellae interplay with host cells. Nat Rev Microbiol. 2008;6(1):53-66.
6. Deng Z, Hou K, Valencak TG, Luo XM, Liu J, Wang H. AI-2/LuxS Quorum Sensing System Promotes Biofilm Formation of Lactobacillus rhamnosus GG and Enhances the Resistance to Enterotoxigenic Escherichia coli in Germ-Free Zebrafish. Microbiol Spectr. 2022;10(4):e0061022.
7. Do H, Makthal N, VanderWal AR, Saavedra MO, Olsen RJ, Musser JM, et al. Environmental pH and peptide signaling control virulence of Streptococcus pyogenes via a quorum-sensing pathway. Nat Commun. 2019;10(1):2586.
8. Moslehi-Jenabian S, Gori K, Jespersen L. AI-2 signalling is induced by acidic shock in probiotic strains of Lactobacillus spp. International journal of food microbiology. 2009;135(3):295-302.
9. Gu Y, Wu J, Tian J, Li L, Zhang B, Zhang Y, et al. Effects of Exogenous Synthetic Autoinducer-2 on Physiological Behaviors and Proteome of Lactic Acid Bacteria. ACS omega. 2020;5(3):1326-35.
10. Miller ST, Xavier KB, Campagna SR, Taga ME, Semmelhack MF, Bassler BL, et al. Salmonella typhimurium recognizes a chemically distinct form of the bacterial quorum-sensing signal AI-2. Mol Cell. 2004;15(5):677-87.
11. Xavier KB, Bassler BL. Regulation of uptake and processing of the quorum-sensing autoinducer AI-2 in Escherichia coli. Journal of bacteriology. 2005;187(1):238-48.
12. Vendeville A, Winzer K, Heurlier K, Tang CM, Hardie KR. Making 'sense' of metabolism: autoinducer-2, LuxS and pathogenic bacteria. Nat Rev Microbiol. 2005;3(5):383-96.
13. Chatterjee R, Shreenivas MM, Sunil R, Chakravortty D. Enteropathogens: Tuning Their Gene Expression for Hassle-Free Survival. Frontiers in microbiology. 2018;9:3303.
14. Choi J, Park J, Ryu S. Repressed Quorum sensing by overexpressing LsrR Hampers Salmonella evasion from oxidative killing within macrophages. J Microbiol Biotechnol. 2010;20(12):1624-9.
15. Choi J, Shin D, Kim M, Park J, Lim S, Ryu S. LsrR-mediated quorum sensing controls invasiveness of Salmonella typhimurium by regulating SPI-1 and flagella genes. PloS one. 2012;7(5):e37059.
16. Choi J, Shin D, Ryu S. Implication of quorum sensing in Salmonella enterica serovar typhimurium virulence: the luxS gene is necessary for expression of genes in pathogenicity island 1. Infect Immun. 2007;75(10):4885-90.
17. Pradhan D, Devi Negi V. Stress-induced adaptations in Salmonella: A ground for shaping its pathogenesis. Microbiol Res. 2019;229:126311.
18. Janssens JC, Steenackers H, Robijns S, Gellens E, Levin J, Zhao H, et al. Brominated furanones inhibit biofilm formation by Salmonella enterica serovar Typhimurium. Appl Environ Microbiol. 2008;74(21):6639-48.

19. Pan J, Bahar AA, Syed H, Ren D. Reverting antibiotic tolerance of Pseudomonas aeruginosa PAO1 persister cells by (Z)-4-bromo-5-(bromomethylene)-3-methylfuran-2(5H)-one. PloS one. 2012;7(9):e45778.
20. Rutherford ST, Bassler BL. Bacterial quorum sensing: its role in virulence and possibilities for its control. Cold Spring Harb Perspect Med. 2012;2(11).
21. Jesudhasan PR, Cepeda ML, Widmer K, Dowd SE, Soni KA, Hume ME, et al. Transcriptome analysis of genes controlled by luxS/autoinducer-2 in Salmonella enterica serovar Typhimurium. Foodborne Pathog Dis. 2010;7(4):399-410.
22. Bearson BL, Wilson L, Foster JW. A low pH-inducible, PhoPQ-dependent acid tolerance response protects Salmonella typhimurium against inorganic acid stress. Journal of bacteriology. 1998;180(9):2409-17.
23. Lang C, Zhang Y, Mao Y, Yang X, Wang X, Luo X, et al. Acid tolerance response of Salmonella during simulated chilled beef storage and its regulatory mechanism based on the PhoP/Q system. Food Microbiol. 2021;95:103716.
24. Jung K, Fabiani F, Hoyer E, Lassak J. Bacterial transmembrane signalling systems and their engineering for biosensing. Open Biol. 2018;8(4).
25. Chakraborty S, Winardhi RS, Morgan LK, Yan J, Kenney LJ. Non-canonical activation of OmpR drives acid and osmotic stress responses in single bacterial cells. Nat Commun. 2017;8(1):1587.
26. Abramson J, Adler J, Dunger J, Evans R, Green T, Pritzel A, et al. Addendum: Accurate structure prediction of biomolecular interactions with AlphaFold 3. Nature. 2024;636(8042):E4.
27. Schmid EW, Walter JC. Predictomes: A classifier-curated database of AlphaFold-modeled protein-protein interactions. bioRxiv. 2024.
28. Baker FN, Porollo A. CoeViz: a web-based tool for coevolution analysis of protein residues. BMC Bioinformatics. 2016;17:119.
29. Liew ATF, Foo YH, Gao Y, Zangoui P, Singh MK, Gulvady R, et al. Single cell, super-resolution imaging reveals an acid pH-dependent conformational switch in SsrB regulates SPI-2. Elife. 2019;8.
30. Curtis MM, Sperandio V. A complex relationship: the interaction among symbiotic microbes, invading pathogens, and their mammalian host. Mucosal Immunol. 2011;4(2):133-8.
31. Papenfort K, Bassler BL. Quorum sensing signal-response systems in Gram-negative bacteria. Nat Rev Microbiol. 2016;14(9):576-88.
32. Oliveira RA, Cabral V, Torcato I, Xavier KB. Deciphering the quorum-sensing lexicon of the gut microbiota. Cell Host Microbe. 2023;31(4):500-12.
33. Thompson JA, Oliveira RA, Djukovic A, Ubeda C, Xavier KB. Manipulation of the quorum sensing signal AI-2 affects the antibiotic-treated gut microbiota. Cell reports. 2015;10(11):1861-71.
34. Lagkouvardos I, Lesker TR, Hitch TC, Gálvez EJ, Smit N, Neuhaus K, et al. Sequence and cultivation study of Muribaculaceae reveals novel species, host preference, and functional potential of this yet undescribed family. Microbiome. 2019;7:1-15.
35. Xiao Y, Zou H, Li J, Song T, Lv W, Wang W, et al. Impact of quorum sensing signaling molecules in gram-negative bacteria on host cells: current understanding and future perspectives. Gut Microbes. 2022;14(1):2039048.
36. Thompson JA, Oliveira RA, Xavier KB. Chemical conversations in the gut microbiota. Gut Microbes. 2016;7(2):163-70.
37. Dethlefsen L, Huse S, Sogin ML, Relman DA. The pervasive effects of an antibiotic on the human gut microbiota, as revealed by deep 16S rRNA sequencing. PLoS Biol. 2008;6(11):e280.
38. Thompson JA, Oliveira RA, Djukovic A, Ubeda C, Xavier KB. Manipulation of the quorum sensing signal AI-2 affects the antibiotic-treated gut microbiota. Cell Rep. 2015;10(11):1861-71.

39. Herzog MK-M, Peters A, Shayya N, Cazzaniga M, Kaka Bra K, Arora T, et al. Comparing Campylobacter jejuni to three other enteric pathogens in OligoMM12 mice reveals pathogen-specific host and microbiota responses. Gut Microbes. 2025;17(1):2447832.
40. Brugiroux S, Beutler M, Pfann C, Garzetti D, Ruscheweyh H-J, Ring D, et al. Genome-guided design of a defined mouse microbiota that confers colonization resistance against Salmonella enterica serovar Typhimurium. Nature microbiology. 2016;2(2):1-12.
41. Xavier KB, Bassler BL. Interference with AI-2-mediated bacterial cell-cell communication. Nature. 2005;437(7059):750-3.
42. Li H, Wang H, D'Aoust JY, Maurer J. Salmonella species. Food microbiology: fundamentals and frontiers. 2012:223-61.
43. Ha JH, Hauk P, Cho K, Eo Y, Ma X, Stephens K, et al. Evidence of link between quorum sensing and sugar metabolism in Escherichia coli revealed via cocrystal structures of LsrK and HPr. Science advances. 2018;4(6):eaar7063.
44. Rychlik I, Barrow PA. Salmonella stress management and its relevance to behaviour during intestinal colonisation and infection. FEMS Microbiol Rev. 2005;29(5):1021-40.
45. Chakravortty D, Rohde M, Jager L, Deiwick J, Hensel M. Formation of a novel surface structure encoded by Salmonella Pathogenicity Island 2. The EMBO journal. 2005;24(11):2043-52.
46. Yu XJ, McGourty K, Liu M, Unsworth KE, Holden DW. pH sensing by intracellular Salmonella induces effector translocation. Science. 2010;328(5981):1040-3.
47. Sridhar S, Steele-Mortimer O. Inherent Variability of Growth Media Impacts the Ability of Salmonella Typhimurium to Interact with Host Cells. PloS one. 2016;11(6):e0157043.
48. Nair AV, Singh A, Devasurmutt Y, Rahman SA, Tatu US, Chakravortty D. Spermidine constitutes a key determinant of motility and attachment of Salmonella Typhimurium through a novel regulatory mechanism. Microbiol Res. 2024;281:127605.
49. Datsenko KA, Wanner BL. One-step inactivation of chromosomal genes in Escherichia coli K-12 using PCR products. Proceedings of the National Academy of Sciences of the United States of America. 2000;97(12):6640-5.
50. Nair AV, Singh A, Rajmani R, Chakravortty D. Salmonella Typhimurium employs spermidine to exert protection against ROS-mediated cytotoxicity and rewires host polyamine metabolism to ameliorate its survival in macrophages. Redox Biology. 2024;72:103151.
51. Sakoh H, Sakuraba S, Sugimoto Y, Imamura H, Jona H, Yamada K, et al. Synthesis and antifungal activity of novel 14-membered benzomacrolides, as galbonolide analogues. Chemical and pharmaceutical bulletin. 2004;52(1):163-5.
52. Miyawaki K, Takagi T, Shibakami M. Efficient synthesis of parallel cyclobolaphiles having two diacetylenes: mimetics of archaeal membrane lipids. Synlett. 2002;2002(08):1326-8.
53. Gardner PM, Winzer K, Davis BG. Sugar synthesis in a protocellular model leads to a cell signalling response in bacteria. Nature chemistry. 2009;1(5):377-83.
54. De Keersmaecker SC, Varszegi C, van Boxel N, Habel LW, Metzger K, Daniels R, et al. Chemical synthesis of (S)-4, 5-dihydroxy-2, 3-pentanedione, a bacterial signal molecule precursor, and validation of its activity in Salmonella typhimurium. Journal of Biological Chemistry. 2005;280(20):19563-8.
55. Surette MG, Miller MB, Bassler BL. Quorum sensing in Escherichia coli, Salmonella typhimurium, and Vibrio harveyi: a new family of genes responsible for autoinducer production. Proceedings of the National Academy of Sciences of the United States of America. 1999;96(4):1639-44.
56. Allam US, Krishna MG, Sen M, Thomas R, Lahiri A, Gnanadhas DP, et al. Acidic pH induced STM1485 gene is essential for intracellular replication of Salmonella. Virulence. 2012;3(2):122-35.
57. Shen Y, Rosendale M, Campbell RE, Perrais D. pHuji, a pH-sensitive red fluorescent protein for imaging of exo- and endocytosis. J Cell Biol. 2014;207(3):419-32.

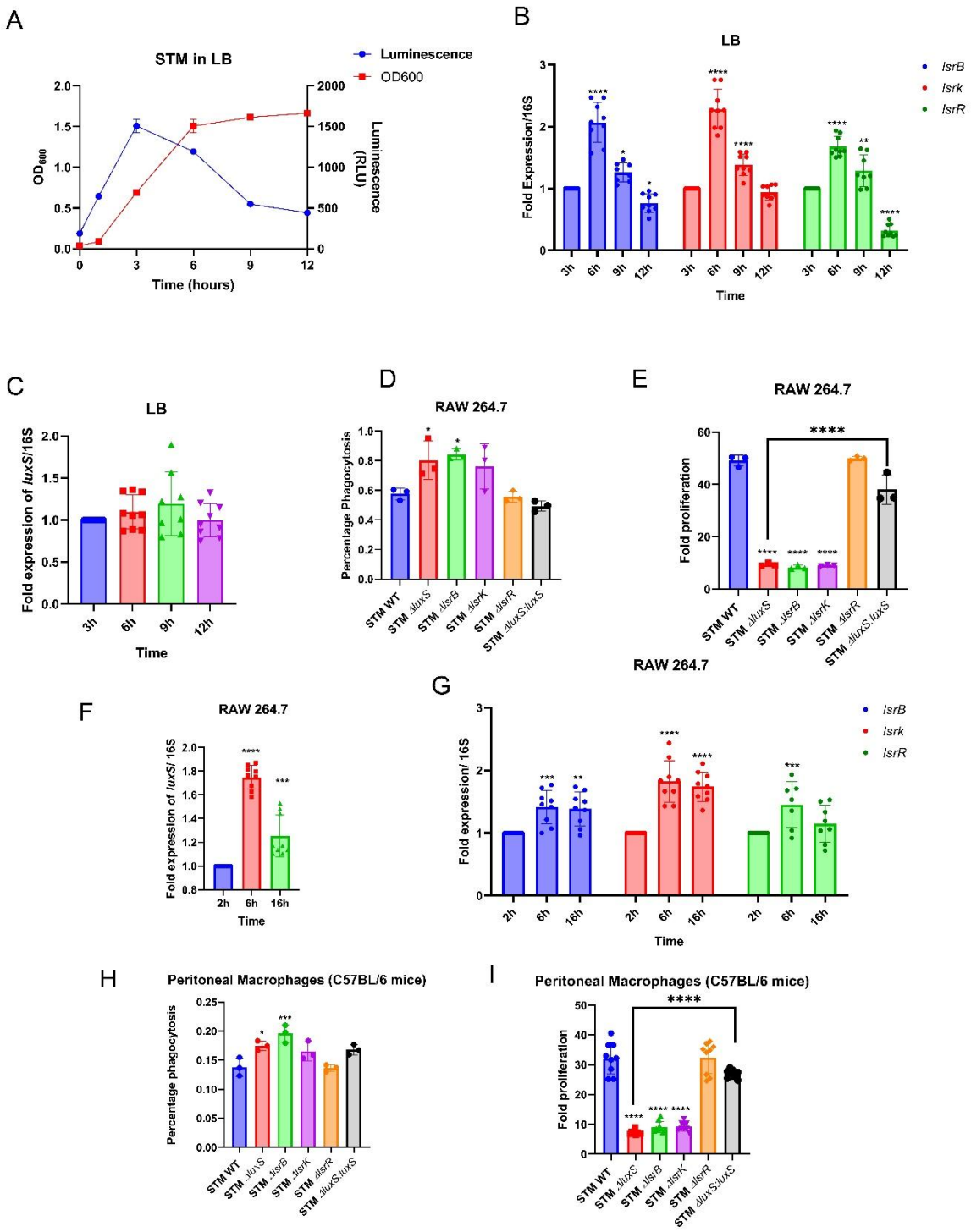

Fig.1: **LuxS/AI-2 quorum sensing is required by *Salmonella* Typhimurium to survive in the macrophages. (A)** *Salmonella* growth with AI-2 production in LB media. Represented as Mean±SD of N=3, n=4, **(B)** The mRNA expression of *lsr* operon genes *lsrB*, *lsrK*, and *lsrR* and **(C)** *luxS* gene expression in STM WT *in vitro* growth in LB. Represented as Mean±SD of N=3,

n=3, **(D)** Percentage phagocytosis, and **(E)** Fold proliferation upon infection in RAW 264.7 macrophages. Represented as Mean±SEM of N=3, n=3, **(F)** *luxS* gene **(G)** *lsr* operon gene *lsrB*, *lsrk*, and *lsrR* expression in STM WT upon infection in RAW264.7 macrophages. Represented as Mean±SD of N=3, n=3 **(H)** Percentage phagocytosis and **(I)** Fold proliferation, upon infection in peritoneal macrophages. Represented as Mean±SEM of N=3, n=3. One-way ANOVA with Dunnet's post-hoc test was used to analyze the data; p values **** $p < 0.0001$, *** $p < 0.001$, ** $p<0.01$, * $p<0.05$. Two-way Anova was used to analyze the grouped data; p values **** $p < 0.0001$, *** $p < 0.001$, ** $p<0.01$, * $p<0.05$

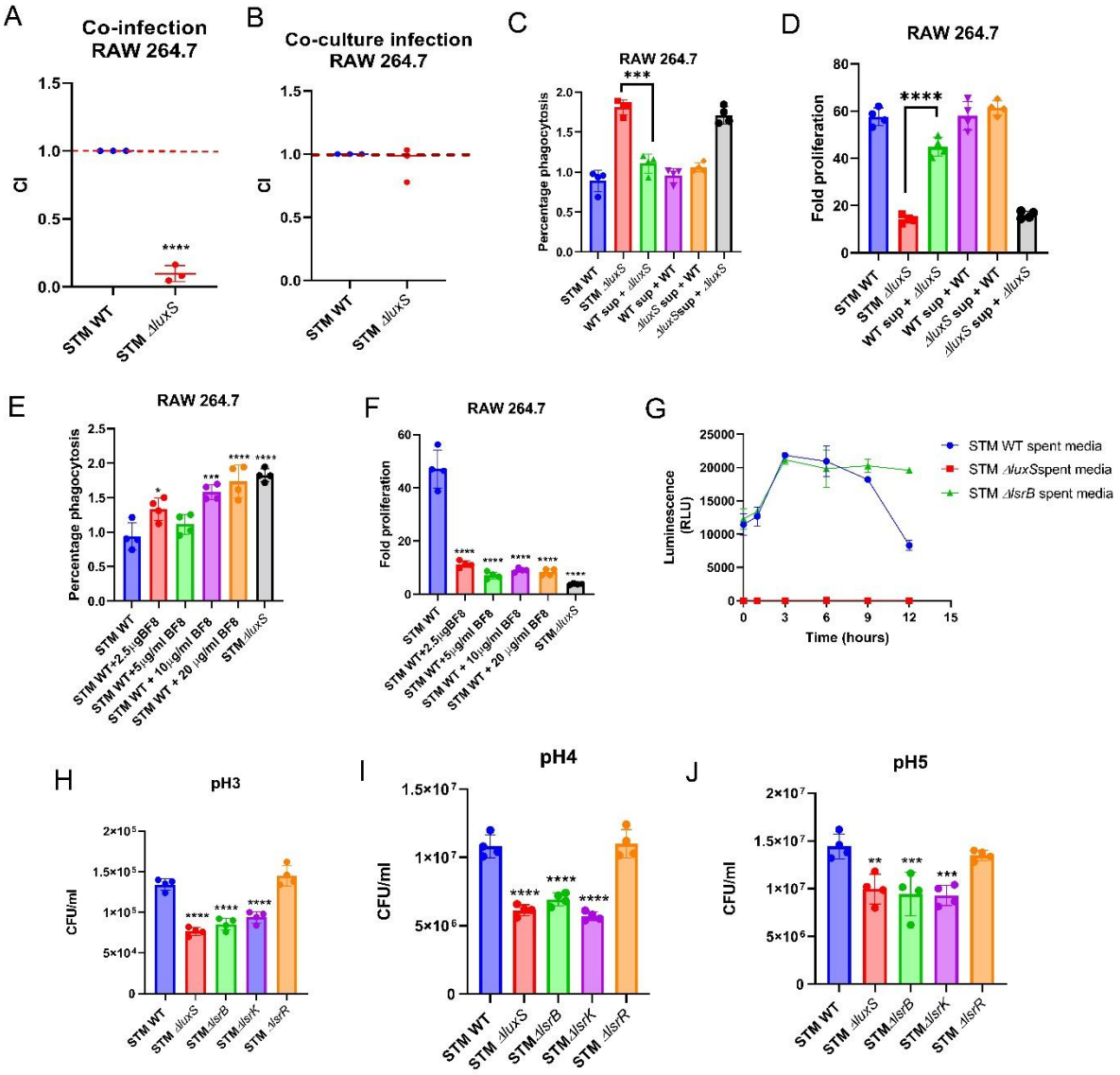

Fig. 2: STM Δ*luxS* acquires AI-2 from STM WT during its *in vitro* growth but not do so within its intravacuolar niche (A) Co-infection assay between STM WT and STMΔ*luxS upon* infection in RAW 264.7 macrophages at the ratio 1:1. Represented as Mean±SEM of N=3, n=3, **(B)** Co-culture grown STM WT and STMΔ*luxS* followed by infection in RAW 264.7 macrophages. Represented as Mean±SEM of N=3, n=3, **(C)** Percentage phagocytosis, **(D)** Fold proliferation of STM in RAW 264.7 macrophages upon 50% spent media treatment of STM WT and STMΔ*luxS*. Represented as Mean±SD of N=3, n=3, **(E)** Percentage phagocytosis, **(F)** Fold proliferation of STM in RAW 264.7

macrophages upon treatment of BF-8 inhibitor. Represented as Mean±SD of N=3, n=3. **(G)** AI-2 production by STM WT, STMΔ*luxS*, and STMΔ*lsrB* in F-media (pH 5). Represented as Mean±SD of N=3, n=3. STM WT, STM*ΔluxS*, STM*ΔlsrB*, STM*ΔlsrK,* and STM*ΔlsrR* survival in different ranges of pH(3-8) of PBS (H), pH 3 survival, **(I)** pH 4 survival, **(J)** pH 5 survival. Unpaired Student's t-test was used to analyze the data; **** $p < 0.0001$, *** $p < 0.001$, ** $p<0.01$, * $p<0.05$. One-way ANOVA with Dunnet's post-hoc test was used to analyze the data; p values **** $p < 0.0001$, *** $p < 0.001$, ** $p<0.01$, * $p<0.05$

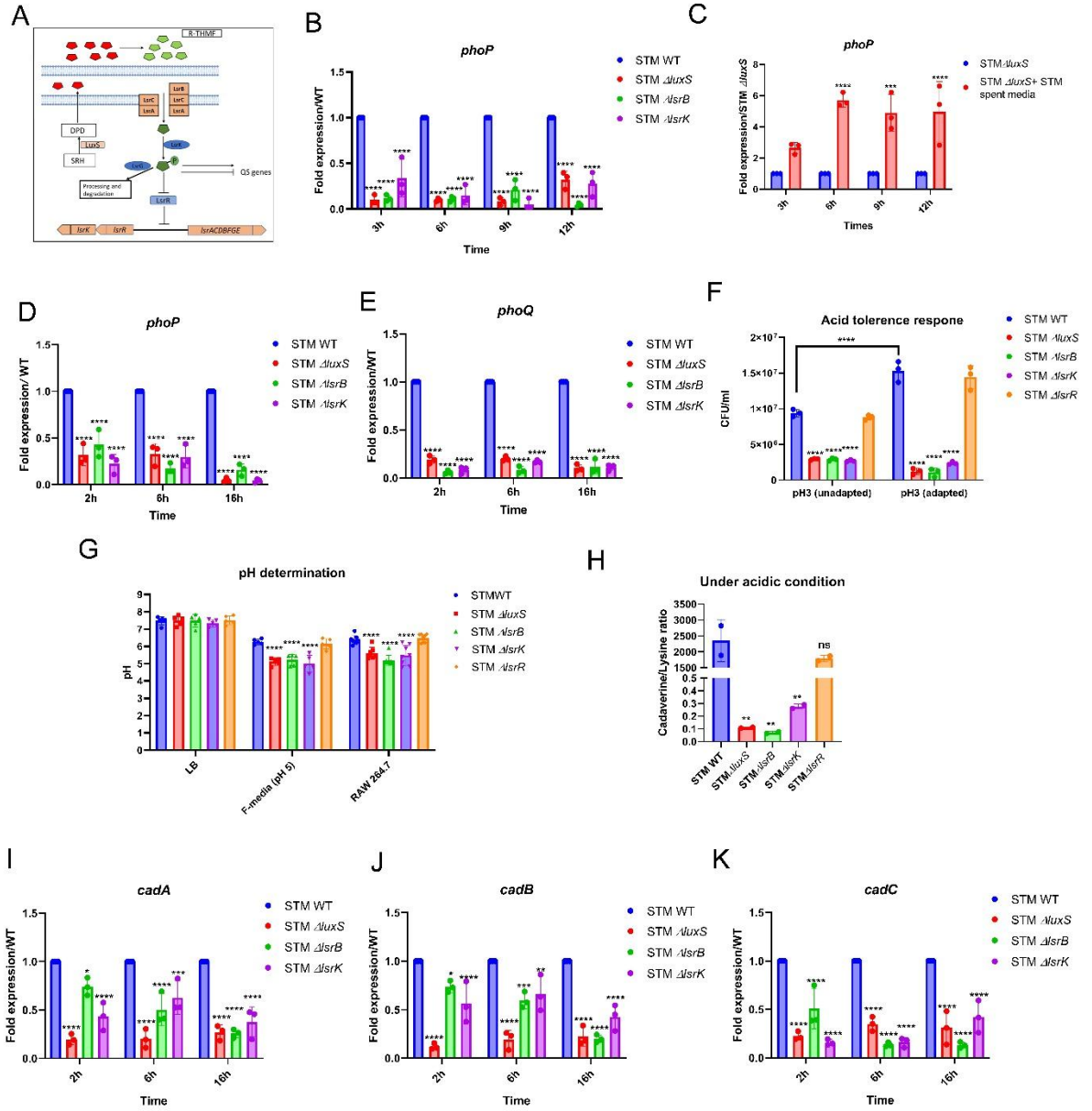

Fig. 3: LuxS/AI-2 system tunes *phoP* expression, thereby assisting in pH sensing and adaptation in *Salmonella*. (A) Schematic of AI-2 synthesis and processing in *Salmonella* Typhimurium. **(B)** *phoP* gene expression in STM WT, STM*ΔluxS*, STM*ΔlsrB*, and STM*ΔlsrK in vitro* conditions LB media. Represented as Mean±SD of N=3, n=3. **(C)** mRNA expression of *phoP in* STM*ΔluxS* upon treatment of STM WT spent media. Represented as Mean±SD of N=3, n=3. **(D)** *phoP* **(E)** *phoQ* expression in STM WT, STM*ΔluxS*, STM*ΔlsrB*, and STM*ΔlsrK* upon infection in RAW 264.7 macrophages. Represented as Mean±SD of N=3, n=3. **(F)** STM WT, STM*ΔluxS*, STM*ΔlsrB*,

STM*ΔlsrK*, and STM*ΔlsrR* acid adaptation and tolerance. Represented as Mean±SD of N=3, n=3. **(G)** Cytosolic pH determination of STM WT, STM*ΔluxS*, STM*ΔlsrB*, STM*ΔlsrK*, and STM*ΔlsrR* by phuji plasmid in LB Media, in F-media (pH 5) and upon infection RAW 264.7 macrophages. Represented as Mean±SD of N=3, n=4. **(H)** Ratio of cadaverine and lysine under acidic conditions (pH 5), N=2. **(I)** *cadA*, (**J)** *cadB,* and **(K)** *cadC*, mRNA expression upon infection in RAW 264.7 macrophages. Represented as Mean±SD of N=3, n=3. One-way ANOVA with Dunnet's post-hoc test was used to analyze the data; p values **** $p < 0.0001$, *** $p < 0.001$, ** $p<0.01$, * $p<0.05$. Two-way ANOVA was used to analyze the grouped data; p values **** $p < 0.0001$, *** $p < 0.001$, ** $p<0.01$, * $p<0.05$

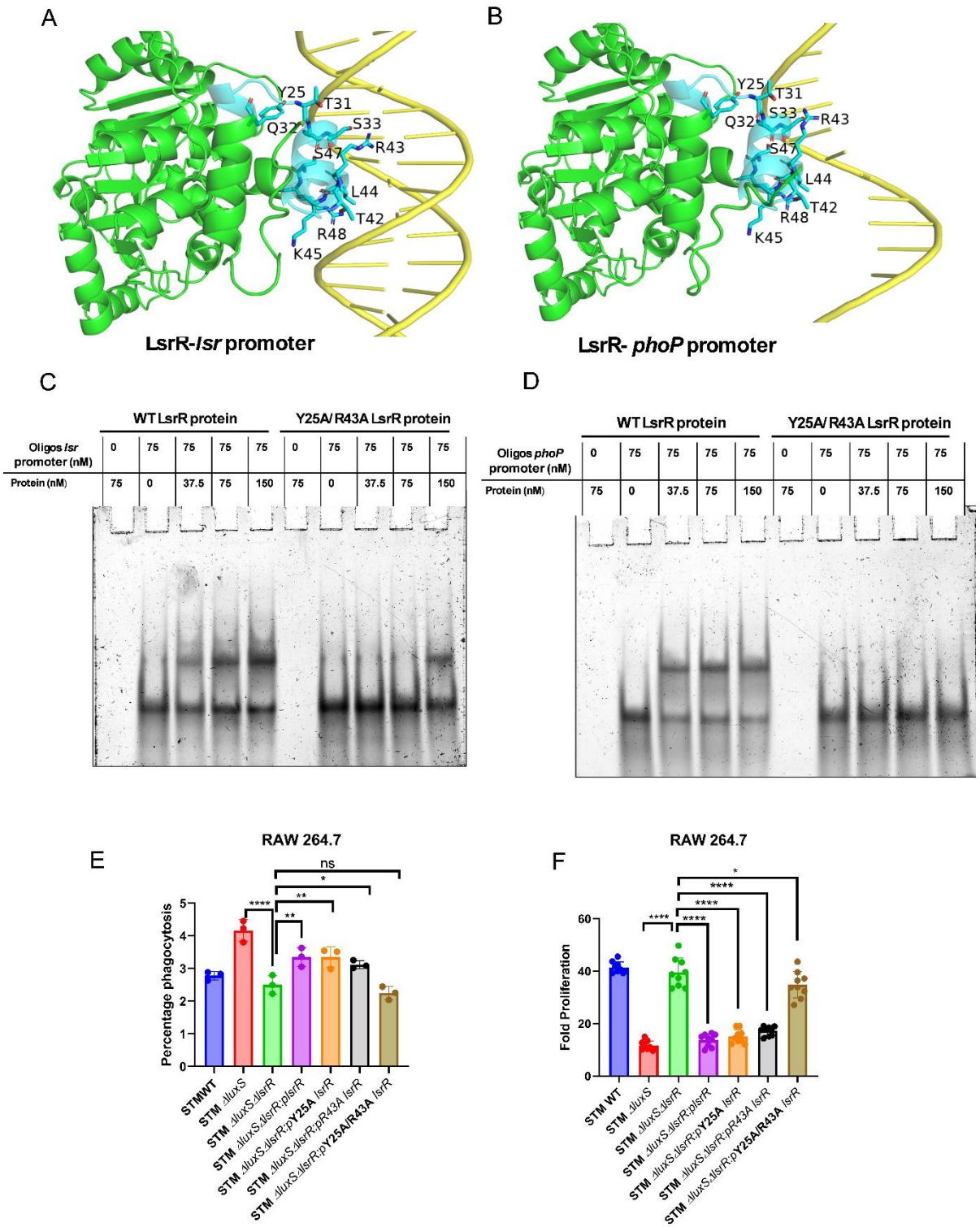

Fig. 4: LuxS/AI-2 signaling regulates *phoP/phoQ* expression through LsrR interaction with the *phoP* promoter in *Salmonella*. AlphaFold3 structural models visualised using pymol depicting LsrR (green) interactions with the *phoP* and *lsr* promoters (yellow). The N-terminal domain residues, spanning

helices 1, 2, and 3, are highlighted in blue, and the key interacting residues of LsrR are represented with a ball and stick model **(A, B)**. Electrophoretic mobility shift assays (EMSA) assessing DNA binding of wild-type LsrR and its Y25A/R43A mutant to *lsr* and *phoP* promoters (**C, D)**. Intracellular survival assay (ICSA) with mutated Y25A, R43A, and Y25A/R43A *lsrR* cloned in pQE-60 complemented strains **(E)** phagocytosis and **(F)** Fold proliferation. Represented as Mean±SD of N=3, n=3. One-way ANOVA with Dunnet's post-hoc test was used to analyze the data; p values **** $p < 0.0001$, *** $p < 0.001$, ** $p<0.01$, * $p<0.05$.

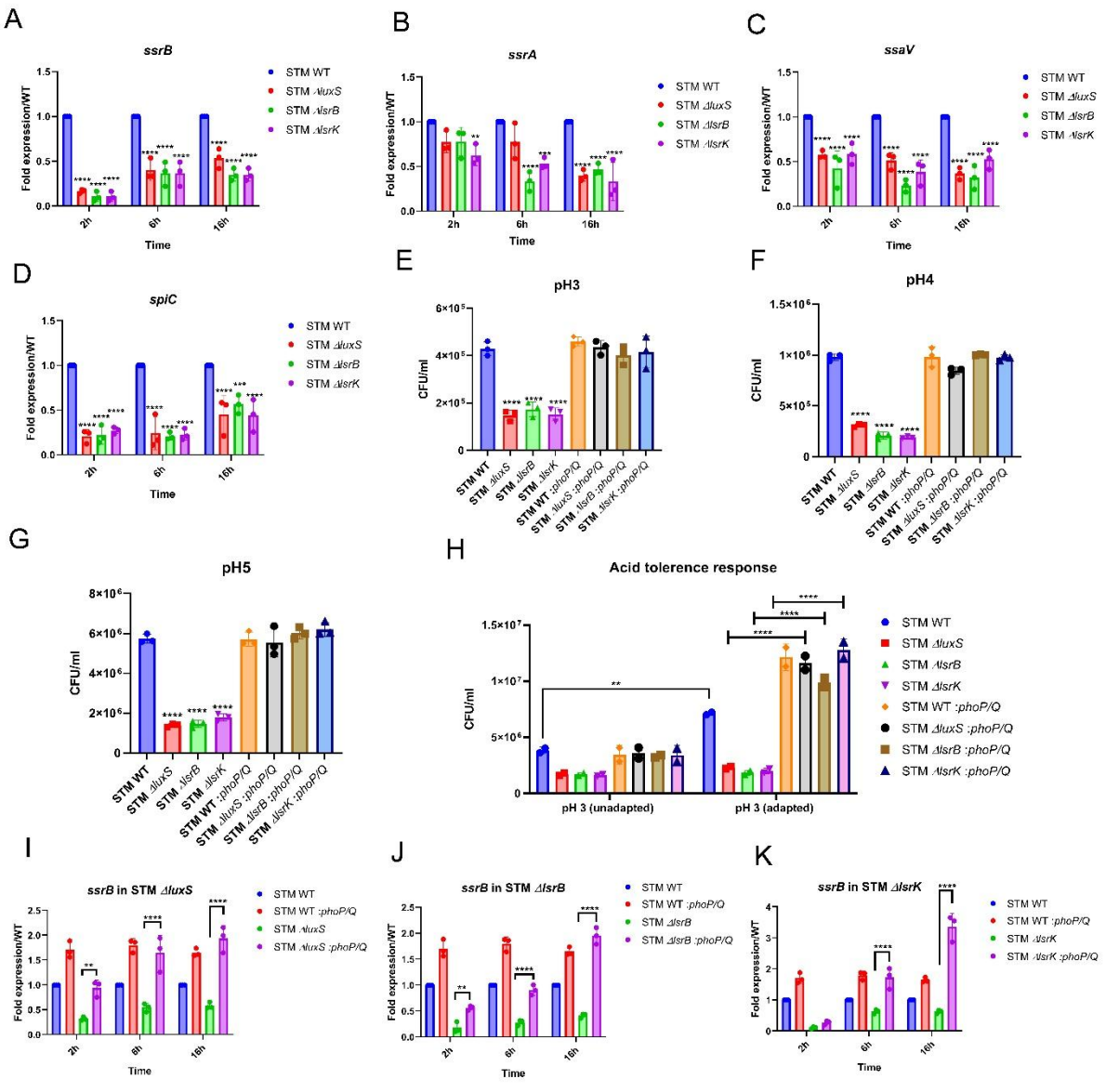

Fig. 5: AI-2 orchestrates the *Salmonella* pathogenicity island-2 gene expression by sensing low pH. (A)*ssrB* **(B)** *ssrA* **(C)** *ssaV* **(D)** *spiC,* mRNA expression in STM WT, STM*ΔluxS*, STM*ΔlsrB*, and STM*ΔlsrK* upon infection in RAW 264.7 macrophages. Represented as Mean±SD of N=3, n=3. STM WT, STM*ΔluxS*, STM*ΔlsrB*, STM*ΔlsrK,* STM WT: *phoP*, STM*ΔluxS*: *phoP*, STM*ΔlsrB*: *phoP*, STM*ΔlsrK*: *phoP* survival in PBS at **(E)** pH3, **(F)** pH4, **(G)** pH5. Represented as Mean±SD of N=3, n=2. **(H)** STM WT, STM*ΔluxS*, STM*ΔlsrB*, STM*ΔlsrK,* STM WT:*phoP*, STM*ΔluxS*:*phoP*, STMΔlsrB:*phoP*, STM*ΔlsrK*: *phoP*

1044 acid adaptation and tolerance. Represented as Mean±SD of N=3, n=2. *ssrB*
1045 mRNA expression in *phoP*/*phoQ* cloned strain of **(I)** STM*ΔluxS,* **(J)** STM*ΔlsrB*
1046 and **(K)** STM*ΔlsrK*. Represented as Mean±SD of N=3, n=3. One-way ANOVA
1047 with Dunnet's post-hoc test was used to analyze the data; p values **** $p <$
1048 0.0001, *** $p < 0.001$, ** $p<0.01$, * $p<0.05$. Two-way ANOVA was used to
1049 analyze the grouped data; p values **** $p < 0.0001$, *** $p < 0.001$, ** $p<0.01$,
1050 * $p<0.05$

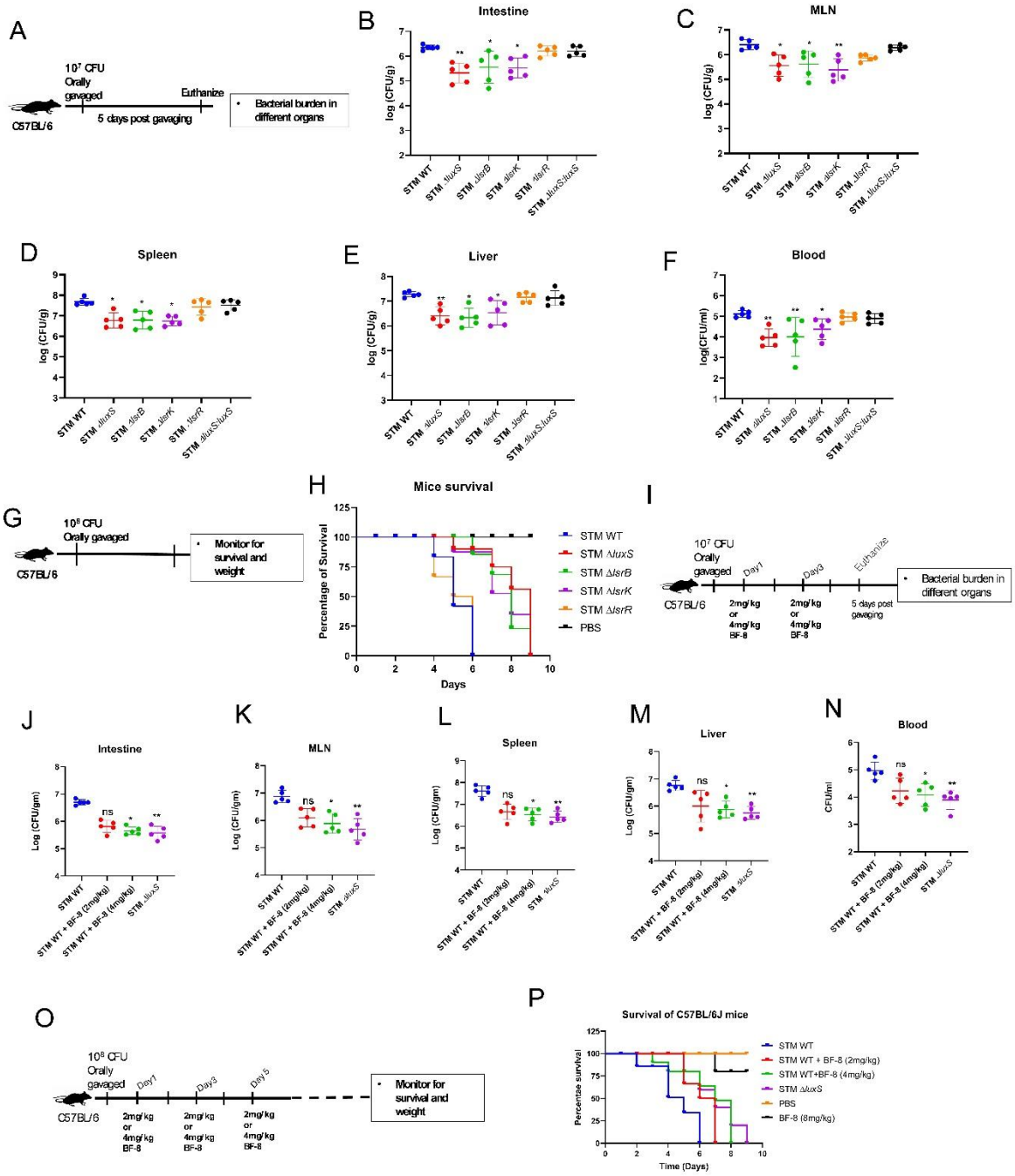

Fig. 6: The absence of AI-2 mediated signaling compromises the *in vivo* colonization of *Salmonella*. (A) The experimental protocol for organ burden in C57BL/6J mice by orally gavaging 10^7 CFU per mouse. The organ burden post 5 days of oral gavage in **(B)** Intestine, **(C)**Mesenteric lymph node (MLN), **(D)** Spleen, **(E)** Liver, and dissemination in **(F)** Blood. Represented as Mean±SD of N=2, n=5 **(G)** The experimental protocol for C57BL/6J mice

survival by orally gavaging 10^8 CFU of STM per mouse. **(H)** Percentage survival of Mice upon infection with STM WT, STM*ΔluxS*, STM*ΔlsrB*, STM*ΔlsrK,* STM*ΔlsrR* and STM*ΔluxS:luxS*. (**I)** The experimental protocol for organ burden in C57BL/6J mice by orally gavaging 10^7 CFU per mouse upon treatment of BF-8 inhibitor (2mg/kg and 4mg/kg through the Intraperitoneal route). The organ burden post 5 days of oral gavage in **(J)** Intestine, **(K)**Mesenteric lymph node (MLN), **(L)** Spleen, **(M)** Liver, and blood dissemination in **(N)** Blood. Represented as Mean±SD of N=2, n=5. **(O)** The experimental protocol of mice survival in C57BL/6J mice by orally gavaging 10^8 CFU per mouse upon treatment of BF-8 inhibitor (2mg/kg and 4mg/kg through the Intraperitoneal route). **(P)** Percentage survival of Mice upon infection with STM WT, STM WT upon treatment, and STM*ΔluxS*. Non-parametric One-way ANOVA (Kruskal Wallis) with Dunn's posthoc test was used to analyze organ burden in mice.